Three-dimensional mapping of brainstem functional lesions

M. Capozza[1]   G. D. Iannetti[1]   M. Mostarda[2]   G. Cruccu[1,3]
N. Accornero[1]

[1]Department of Neurosciences, University of Rome "La Sapienza", Italy
[2]Institute of Clinical Neurology, University of Rome "La Sapienza", Italy
[3]Neuromed Institute, Pozzilli, Italy

Abstract—*The human brainstem is a highly complex structure where even small lesions can give rise to a variety of symptoms and outward signs. Localising the area of dysfunction within the brainstem is often a difficult task. To make localisation easier, a neural net system has been developed which uses 72 clinical and neurophysiological data inputs to provide a display (using 5268 voxels) on a three-dimensional model of the human brainstem. The net was trained by means of a back-propagation algorithm, over a pool of 580 example cases. Assessed on 200 test cases, the net correctly localised 83.6% of the target voxels; furthermore the net correctly localised the lesions in 31 out of 37 patients. Because this computer-assisted method provides reliable and quantitative localisation of brainstem areas of dysfunction and can be used as a 3D interactive functional atlas, it is expected to prove useful as a diagnostic tool for assessing focal brainstem lesions.*

Keywords—*Brainstem, Neural network, 3D mapping, Neuroimaging, Neurophysiological tests*

1 Introduction

THE HUMAN brainstem is a small structure that performs hundreds of functions. Here, in closely arranged groups lie the nuclei and rootlets of the cranial nerves, and the long pathways interconnecting the brain, cerebellum, and spinal cord. Focal lesions in the brainstem can give rise to an array of symptoms and outward signs. In clinical practice, localising a brainstem lesion is often a hard task even for an expert neurologist. Although magnetic resonance imaging (MRI) is helpful, areas of abnormal MRI signal do not necessarily imply tissue damage or dysfunction. Conversely, areas of actual dysfunction may escape MRI detection. The functional correlation of MRI findings is notably poor in inflammatory diseases of the brainstem (ORMEROD *et al.*, 1984; CAPRA *et al.*, 1989; TURANO *et al.*, 1991). Neurophysiological investigations (evoked potentials and trigeminal reflexes) add important topodiagnostic information not obtainable by clinical examination alone (CAPLAN *et al.*, 1993; ONGERBOER DE VISSER and CRUCCU, 1993; HOPF, 1994; KIMURA *et al.*, 1994). But integrating the information from the various neurophysiological tests requires expert neurophysiologists with specialised knowledge of the brainstem (CRUCCU and DEUSCHL, 2000).

Localising the site of brainstem dysfunction is therefore a complex task that encompasses clinical symptoms, neurophysiological responses and the possible involvement of brainstem structures.

Our aim was to solve the clinical problem of integrating all this information to help localise focal brainstem lesions. To do so, a computer-aided tool was developed using a three-dimensional (3D) model of the brainstem and a neural net. A neural net was chosen because connectionist systems have proved valuable in performing arbitrary mapping between highly complex input/output spaces, while exhibiting other desirable properties such as inductive generalisation and gentle degradation (FELDMAN and BALLARD, 1982; RUMELHART *et al.*, 1986; GROSSBERG, 1988; KOHONEN, 1990; SIMPSON, 1990; MILLER *et al.*, 1992; BISHOP, 1995).

2 System architecture

Using data from topometric and stereotactic atlases (SHALTENBRAND and WAHEM, 1977; PAXINOS and HUANG, 1995; KRETSCHMANN and WEINRICH, 1998), we developed an idealised 3D model of the brainstem subdivided into 5268 volume elements ('voxels') ranging from $2 \times 2 \times 2$ mm to $2 \times 2 \times 4$ mm (Fig. 1).

Input to the neural net comprised 72 clinical and neurophysiological data items (see below and Table 1), 36 for the left side of the body and 36 for the right side, each having one of four possible binary values: $00 = $ not available; $01 = $ normal; $10 = $ abnormal; and $11 = $ uncertain. These values were fed into the input layer of the neural net program, which computed and output 5268 floating-point values in the range 0–1 for each of the 5268 voxels. Value 1 stood for a voxel certainly affected by the lesion, value 0 for a voxel certainly unaffected, with fractional values for intermediate probabilities (local probability of lesion, LPL) that the given voxel was affected.
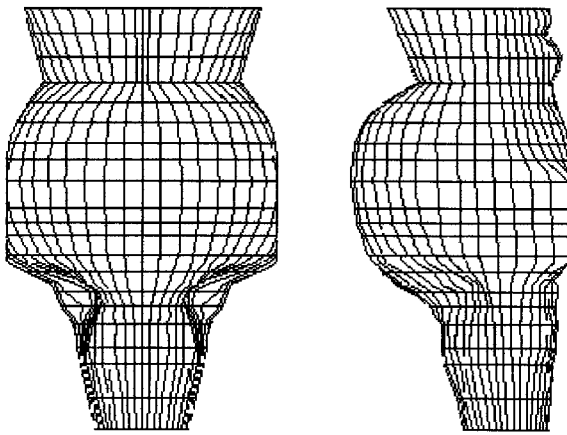
Each voxel was colour-coded according to its LPL and displayed at its proper location in the brainstem model, creating a 3D colour map of the whole functional lesion in the brainstem

Fig. 1 *Framework of the brainstem model; front view (left) and lateral view (right)*

(Fig. 2). This model could be freely rotated and enlarged or reduced ('zoomed') to examine the lesion from any desired angle and apparent distance. From the 3D model, 2D slices could be extracted along any of the three main section planes, and further elaborated graphically to smooth the boundaries (Fig. 3). For pictorial purposes the results can also be exported to a computer-assisted design and/or rendering program, such as Autocad[®] or 3D Studio[®] to be converted into a solid, smooth 3D image.

This software system can be run on any computer with a 24-bit colour display having at least 800 × 600 pixel resolution, under a 32-bit Windows[®] operating system (Windows95[®], Windows98[®], WindowsNT[®]). The network size is about 4 Mb but 16 Mb random access memory is desirable to ensure fast and smooth graphics.

3 Functional input data

Of the 36 input data, 23 were standard clinical signs and symptoms of brainstem dysfunction (Table 1). The 13 neurophysiological items were obtained by trigeminal reflex and evoked potential testing (CAPLAN *et al.*, 1993). The jaw jerk elicited by taps to the chin is a trigemino-trigeminal reflex mediated by a short, unilateral pontomesencephalic circuit (HOPF, 1994; CRUCCU and ONGERBOER DE VISSER, 1999).
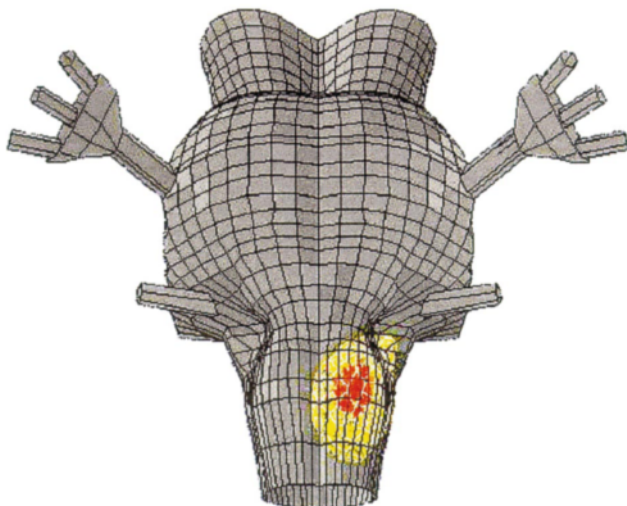
Fig. 2 *3D reconstruction of the functional lesion in a patient with a lateral medullary infarction (Wallenberg's syndrome)*

The masseter inhibitory reflex elicited by perioral electrical stimulations is a trigemino-trigeminal reflex consisting of an early (SP1) and late component (SP2). SP1 is mediated by a short, bilateral, pontine circuit. SP2 is mediated by a long, bilateral, pontomedullary circuit. Impulses for the contralateral response cross at the level of the pontomedullary junction (ONGERBOER DE VISSER *et al.*, 1990; CRUCCU and ONGERBOER DE VISSER, 1999). The blink reflex elicited by electrical stimulation of the supraorbital nerve is a trigemino-facial reflex consisting of an early (R1) and a late (R2) component. R1 is a mediated by a short, unilateral pontine circuit. R2 is mediated by a long, bilateral medullary (down to the caudal medulla-rostral spinal cord) circuit. Impulses cross in the mid medulla, at the level of the obex (ONGERBOER DE VISSER and CRUCCU, 1993; CRUCCU and DEUSCHL, 2000). The brainstem auditory evoked potentials, evoked by acoustic stimuli and recorded from the scalp, consist of several far-field waves: wave III is generated in the lower pons, wave IV in the lateral lemniscus, and wave V in the lower colliculus (DEUSCHL and EISEN, 1999). The motor evoked potentials are elicited in facial and limb muscles by transcranial magnetic stimulation of the motor cortex. The descending volleys travel along the cortico-bulbar and corticospinal tracts in the ventral brainstem (DEUSCHL and EISEN, 1999). The somatosensory evoked potentials are evoked by electrical stimulation of the median or tibial nerves and recorded from the scalp. The ascending volleys travel along the dorsal columns up to the dorsal medulla, then are relayed to the medial lemniscus, cross the midline and ascend in the brainstem tegmentum up to the thalamus (DEUSCHL and EISEN, 1999). Laser evoked potentials are evoked by laser stimulation of the hairy skin. The ascending volleys travel in the spinothalamic tract through the whole caudal-rostral brainstem tegmentum, without crossing the midline (BROMM and TREEDE, 1991; ARENDT-NIELSEN, 1994).

4 Preparation of the example cases and test cases

To train the net, we prepared 780 example cases, representative of the main possible combinations of symptoms and neurophysiological findings, and of the most typical brainstem lesions. All cases had only one focal lesion.

A two-step process was used. First, images of focal brainstem lesions were collected from the existing literature and transposed on the proposed brainstem model. For each case, a local probability of lesion (LPL) was assigned to each voxel on a three-value scale: 0 = unaffected; 0.5 = uncertain; and 1 = affected. These voxels were the target array of the neural net for that case. The input data of each case were also fed with the available clinical-neurophysiological information. Second, the cases (with both the probabilities of lesion and clinical-neurophysiological information) were submitted to three experts in brainstem anatomy and brainstem neurophysiology, who were asked to judge whether the lesion and the functional data of each case were indeed compatible. The cases approved by the experts were finally accepted for the net training.

Of the 780 example cases, 200 were chosen randomly and transferred from the training set to the test set (BISHOP, 1995), the remaining 580 example cases constituted the training set.

5 Network topology and training

We chose a multi-layered, feedforward, fully connected neural network with two hidden layers, trained by back-propagation (RUMELHART *et al.*, 1986).

Table 1 Items of functional input

Clinical examination	Neurophysiological tests
Oculomotor nerve palsy	Jaw jerk
Trochlear nerve palsy	SP1 masseter inhibitory reflex
Abducens nerve palsy	SP1 masseter inhibitory reflex
Internuclear ophthalmoplegia	SP1–SP2 crossed abnormality
Trigeminal hypesthesia	R1 blink reflex
Trigeminal pain	R2 blink reflex (afferent abnormality)
Trigeminal neuralgia	R2 blink reflex (efferent abnormality)
Facial nerve palsy	R2 blink reflex (crossed abnormality)
Hearing disturbances	BAEP* III wave
Dizziness	BAEP* V wave
Lateral propulsion	Motor evoked potentials
Nystagmus	Somatosensory evoked potentials
Rotatory nystagmus	Laser evoked potentials
Nystagmoid movements	
Dysphagia dysphonia dysarthria	
Pharyngeal reflex suppression (unilateral)	
Vocal cord palsy (unilateral)	
Accessory nerve palsy	
Hypoglossal nerve palsy	
Pyramidal syndrome	
Lemniscal sensory disturbance	
Spinothalamic sensory disturbance	
Ataxia	

* BAEP: brainstem auditory evoked potential

The net had 148 input units (because the 74 input data were binary coded), 50 units in the first hidden layer, 150 units in the second hidden layer, and 2634 units in the output layer. By exploiting the functional right–left symmetry of the brainstem and a two-step process, we were able to reduce the output units to one half the 5268 voxels in the model: in a first step, the net, fed with all the right and left input data, computed the output values for the left-sided voxels: in a second step the net was fed with right–left inverted input data, and the output values, right–left inverted, were assigned to the right-sided voxels.

The net used a linear transfer function from the input layer to the first hidden layer and a sigmoid function for the other layers.

The net was trained until every voxel's LPL came within 0.25 of the target value.

To train the net we used the commercial program Qnet® 2.1, which allowed automatic adjustment of the learning rate. On a Pentium II 350 MHz computer, working night and day, training took about one month.

6 Results

When training stopped, the root mean square of the output error had stabilised at a level lower than 0.002. The correlation between the targets and outputs in the training set reached 0.999 (R correlation coefficient).

We also cross-validated the net with the set of 200 'unknown' test cases that had been randomly chosen and excluded from the training set (see above). The LPL error 'e' for each single voxel was computed as: $e = $ output value minus target value. False positive errors ranged from 0 to 1 and false negative errors ranged from 0 to -1. Error frequencies were grouped into classes 0.25 wide (Table 2). More than 80% of voxels (83.6%) showed an absolute error lower than 0.25.

This kind of error evaluation lacks spatial information (see Discussion). To provide information on the spatial errors, we also computed, for any voxel having an output value 'V' with an absolute error higher than 0.25, its spatial distance from the nearest voxel having a target value within ± 0.25 from 'V'. Out

of 173 001 voxels having absolute errors equal to or higher than 0.25, 131 481 (76%) showed a spatial distance of 1 voxel (neighbouring voxels) and 38 060 (22%) a distance of 2 voxels. This distinction suggests that apparently high errors might in reality reflect relatively small spatial displacements in the LPL (98% were located within 2 voxels).

After net validation with the set of test cases, the method was used in a retrospective study of 40 patients from our neurological division. Patients with one focal brainstem lesion were selected and patients with multiple sclerosis or tumours were excluded as they are expected to yield a poor anatomical–functional correlation. The net was fed with the available clinical and neurophysiological data of each case. The 3D functional lesion produced by the net was submitted to the opinion of an expert who compared it with the clinical notes and the available neuroimaging pictures.

The expert judged the output of the net correct in 31 cases. In six cases, only having clinical and neurophysiological signs of impairment of the motor or sensory pathways on one side (unilateral pyramidal or somatosensory syndromes), the net assigned a uniformly low LPL to all the voxels of the involved corticospinal or somatosensory tract. In three cases the expert judged the input data insufficient.

Table 2 Distribution of error frequencies

Error (e)	Number of voxels	Percentage of voxels
$-1 < e \leq -0.75$	0	0
$-0.75 < e \leq -0.50$	15593	1.48
$-0.50 < e \leq -0.25$	93665	8.89
$-0.25 < e < 0$	413117	39.21
$p \leq e < 0.25$	467482	44.37
$0.25 \leq e < 0.50$	55209	5.24
$0.50 \leq e < 0.75$	8534	0.81
$0.75 \leq e < 1$	0	0
Total	1053600	100
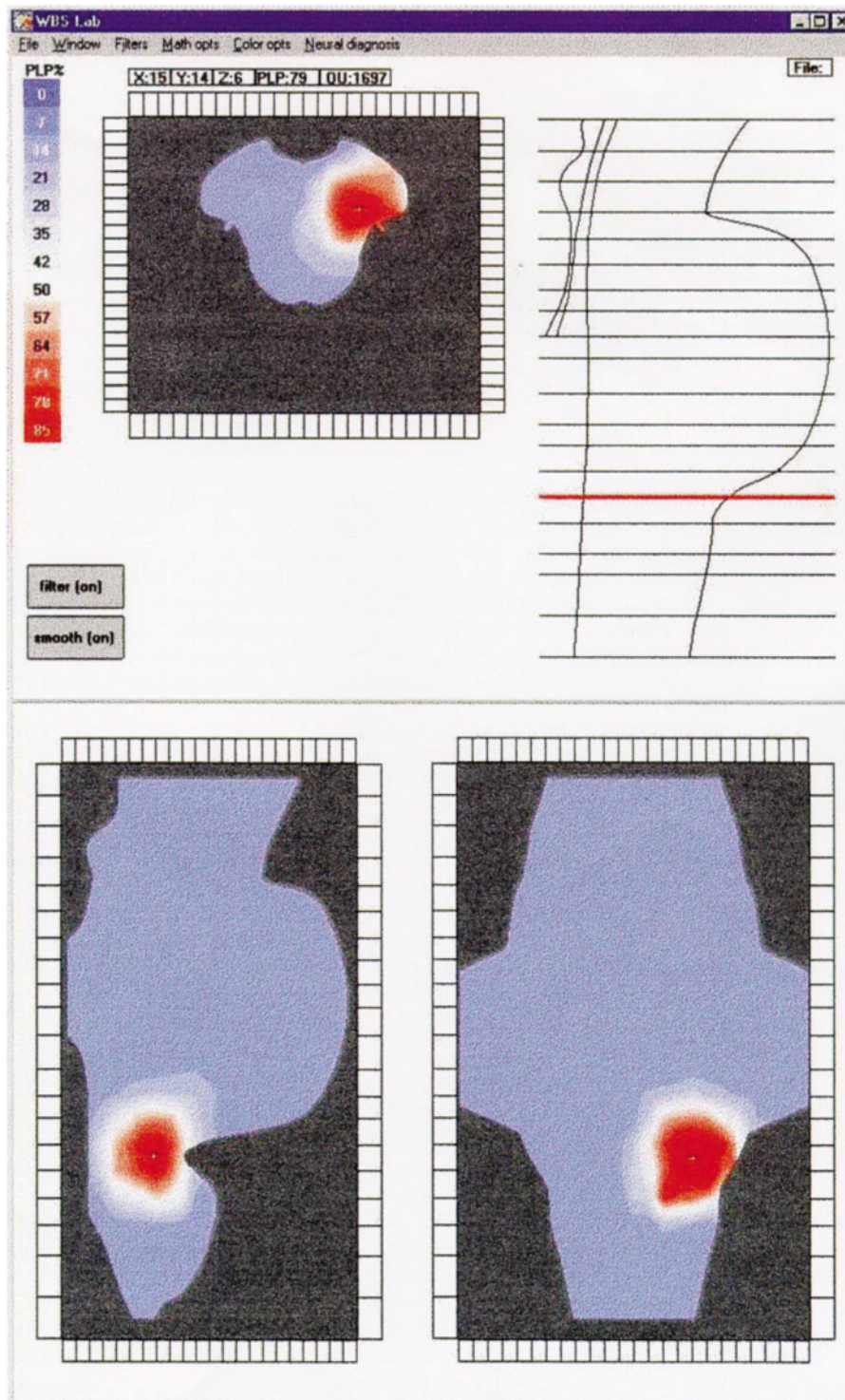
Fig. 3 *Two-dimensional display (after smoothing) on the axial (upper left), sagittal (lower left), and coronal (lower right) planes, of the functional lesion shown in Fig. 2. The thick line on the sagittal frame (upper right) indicates the level of the axial section. The colour scale represents the local probability of lesion (LPL), increasing from blue to red. The cursor in the middle of the red areas indicates the maximum LPL (79%)*

7 Discussion

While neural networks are by no means a novelty in auto-mated diagnostic systems (SHARPE and CALEB, 1994; YANG *et al.*, 1994; ACCORNERO and CAPOZZA, 1995; ARMONI, 1998), the diagnostic task presented is unusual because it entails topographic rather than semantic diagnosis. In conventional diagnostic systems, numerical outputs represent the likelihood that the various nosographic entities considered will be true in the observed subject. In our system, instead of an 'abstract' nosographic probability, each probability had to be assigned a small, well localised spatial point in a nervous system.

Quantitatively, this difference raised the number of outputs from several tens to several thousands. From a conceptual point of view, it also required the diagnostic system to solve interesting problems about the spatial relations among the various outputs. These exigencies led us to decide against a traditional expert system and to use a connectionist system.

To keep the neural net size small a solution was applied that had proved useful in an earlier study (ACCORNERO and CAPOZZA, 1995). Because, unlike the cerebral hemispheres, brainstem functions are right–left symmetric (HARNAD *et al.*, 1977), we decided to use a net that diagnosed only one side of the

brainstem, covering the entire organ by activating the net a second time after exchanging input and output data sides. The number of input units remained unchanged, because the net obviously needed to be 'aware' of the clinical and neurophysiological data from *both* sides of the body at any single activation. This procedure halved the number of output units, thus reducing the amount of memory required. Economy was not the only reason for this arrangement. To a net considering a single side of the brainstem, each example case had a double value, because it provided two examples, one for the left and one for the right side. This resulted in virtually doubling the size of the example set.

The 74 input data were binary coded. Because the input data ranged on four possible categories, each input needed 2 bits and the number of input units was therefore 148. The alternative, coding each datum as a single real number, seemed unacceptable because it would have implied the use of an interval scale to encode the four possible values, i.e. an interval relation between nominal values. After empirical tests using a wide range of values, the number of hidden units was kept as small as possible to facilitate generalisation (ANSHELEVICH *et al.*, 1989; BAUM and HAUSSLER, 1989). The 2634 output units were obviously determined by the number of voxels required for each half of our brainstem model.

A point of importance in assessing the net's performance is that any spatial error may lead to a double LPL error. Let us assume, for example, that a given voxel had a target LPL value of 1, but the net assigned that value to a neighbouring voxel, and a different value to the given voxel. This would result in a double LPL error (one in the given voxel and one in the neighbouring voxel). In this example, the network software correctly computed the LPL quantitatively, but instead of assigning it to the correct voxel erroneously shifted it to a neighbouring voxel. Assessing these spatial errors was difficult, because we had no way of finding out whether the net's LPL for a given voxel was actually a 'shifted' value. Nor could we identify the 'original' voxel for that value, if any. Hence, we had to verify whether any mistaken voxel (i.e. any voxel having an absolute error equal or higher than 0.25) was located within a distance of 1 or 2 voxels from another location where that value would have been acceptable (i.e. absolute error lower than 0.25). This analysis showed that most grossly mistaken voxels were spatial errors from neighbouring voxels (98% when considering neighbours up to a distance of 2 voxels, i.e. 4 mm).

Unlike some other studies designed to solve a clinical problem by applying a neural net approach, in assessing the reliability of the net we could not use real patients as test cases. Traditionally, anatomical–functional correlation studies have always relied on pathological findings. To collect a sufficient number of autopsies was beyond the scope of this study. Furthermore, the wide time interval elapsing between the functional examination and death may corrupt the findings (MASIYAMA *et al.*, 1985; ONGERBOER DE VISSER *et al.*, 1990). Although MRI is far more readily available and timely, it often provides an insufficient correlation between the areas of abnormal signal and the actual areas of dysfunction in the brainstem (BYRNE *et al.*, 1989; CAPRA *et al.*, 1989; CRUCCU and DEUSCHL, 2000). Indeed, the search for a way to overcome the poor ability of MRI in localising and quantifying the *functional* lesion in some diseases prompted us to develop this project. Instead, we relied on net cross-validation with the test cases subtracted from the training set. We also asked an expert to test *qualitatively* how the net performed on a retrospective group of patients with focal brainstem lesions secondary to diseases that are expected to provide a good anatomical/functional correlation. The net performed well. As well as yielding the correct output in most cases it failed only when it received too few data. In particular, when the patient had only dysfunction of the ascending or descending pathways in the ventral brainstem, unaccompanied by a clinical or neurophysio-

logical abnormality indicating the cranial nerves or nuclei or the reflex pathways in the dorsal brainstem, the net could not locate the lesion rostral-caudally and assigned a low probability distributed along the pathway. Human experts have exactly the same difficulty.

In a future study we intend to compare quantitatively the correlation between the areas of abnormal signal yielded by MRI with the areas of dysfunction yielded by our neural network, in patients with ischaemic infarction (expected to provide a good correlation) and in patients with multiple sclerosis (expected to provide a poor correlation).

References

ACCORNERO, N., and CAPOZZA, M. (1995): 'OPTONET: neural network for visual field diagnosis', *Med. Biol. Eng. Comput.*, **33**, pp. 223–226

ANSHELEVICH, V. V., AMIRIKIAN, B. R., LUKASHIN, A. V., and FRANK-KAMENETSKII, M. D. (1989): 'On the ability of neural networks to perform generalization by induction', *Biol. Cybern.*, **61**, pp. 125–128

ARENDT-NIELSEN, L. (1994): 'Characteristics, detection and modulation of laser-evoked vertex potentials', *Acta Anaesthesiol. Scand.*, **38**, pp. 1–36

ARMONI, A. (1998): 'Use of neural networks in medical diagnosis', *MD Comput.*, **15**, (2), pp. 100–104

BAUM, E. B., and HAUSSLER, D. (1989): 'What size net gives valid generalization?' *Neural Comput.*, **1**, (1), pp. 151–160

BISHOP, M. C. (1995): 'Neural networks for pattern recognition' (Oxford University Press, New York)

BROMM, B., and TREEDE, R. D. (1991): 'Laser evoked potentials in the assessment of cutaneous pain sensitivity in normal subjects and patients', *Rev. Neurol.*, **147**, pp. 625–643

BYRNE, J. V., KENDALL, B. E., KINGSLEY, D. P., and MOSELEY, I. F. (1989): 'Lesions of the brain stem: assessment by magnetic resonance imaging', *Neuroradiology*, **31**, (2), pp. 129–133

CAPLAN, L., GUTMANN, L., BESSER, R., and HOPF, H. C. (1993): 'Brain-stem localization and function' (Springer, Heidelberg/New York)

CAPRA, R., MATTIOLI, F., VIGNOLO, L. A., ANTONELLI, A. R., BONFIOLI, F., CAPPIELLO, J., NICOLAI, P., PERETTI, G., and ORLANDINI, A. (1989): 'Lesion detection in MS patients with and without clinical brainstem disorders: magnetic resonance imaging and brainstem auditory evoked potentials compared', *Eur. Neurol.*, **29**, (6), pp. 317–322

CRUCCU, G., and DEUSCHL, G. (2000): 'The clinical use of brainstem reflexes and hand-muscle reflexes', *Clin. Neurophysiol.*, **111**, pp. 371–387

CRUCCU, G., and ONGERBOER DE VISSER, B. W. (1999): 'The jaw reflexes', *Electroencephalogr. Clin. Neurophysiol.*, suppl. **52**, pp. 243–247

DEUSCHL, G., and EISEN, A. (Eds) (1999): 'Recommendations for the practice of clinical neurophysiology: guidelines of the international federation of clinical neurophysiology, 2nd edn, (Elsevier, Amsterdam)

FELDMAN, J., and BALLARD, D. (1982): 'Connectionist models and their properties', *Cognitive Sci.*, **6**, pp. 205–254

GROSSBERG, S. (1988): 'Nonlinear neural networks: principles, mechanisms, and architectures', *Neural Networks*, **1**, pp. 17–61

HARNAD, S. DOTY, R. W., GOLDSTEIN, L., JAYNES, J., and KRAUTHAMER, G. (1977): 'Lateralization in the nervous system' (Academic Press, New York)

HOPF, H. C. (1994): 'Topodiagnostic value of brain stem reflexes', *Muscle Nerve*, **17**, pp. 475–484

KIMURA, J., DAUBE, J., BURKE, D., HALLETT, M., CRUCCU, G., ONGERBOER DE VISSER, B. W., YANAGISAWA, N., SHIMAMURA, M., and ROTHWELL, J. (1994): 'Human reflexes and late responses. Report of an IFCN committee', *Electroencephalogr. Clin. Neurophysiol.*, **90**, pp. 393–403

KOHONEN, T. (1990): 'The self-organizing map', *Proc. IEEE*, **78**, pp. 1464–1480

KRETSCHMANN, H. J., and WEINRICH, W. (1998): 'Neurofunctional systems–3D reconstructions with correlated neuroimaging' (George Thieme Verlag, Stuttgart)

MASIYAMA, S., NIIZUMA, H., and SUZUKI, J. (1985): 'Pontine haemorrhage: a clinical analysis of 26 cases', *J. Neurol. Neurosurg. Psychiatry*, **48**, pp. 658–662

MILLER, A. S., BLOTT, B. H., and HAMES, T. K. (1992): 'Review of neural network applications in medical imaging and signal processing', *Med. Biol. Eng. Comput.*, **30**, pp. 449–464

ONGERBOER DE VISSER, B. W., CRUCCU, G., MANFREDI, M., and KOELMAN, J. H. (1990): 'Effects of brainstem lesions on the masseter inhibitory reflex. Functional mechanisms of reflex pathway', *Brain*, **113**, (3), pp. 781–792

ONGERBOER DE VISSER, B. W., and CRUCCU, G. (1993): 'Neurophysiologic examination of the trigeminal, facial, hypoglossal, and spinal accessory nerves in cranial neuropathies and brain stem disorders' in BROWN, W. F., and BOLTON, C. F. (Eds): 'Clinical electromyography, 2nd edn, (Butterworth-Heinemann, Boston), pp. 61–92

ORMEROD, I. E., ROBERTS, R. C., DU BOULAY, E. P., MCDONALD, W. I., CALLANAN, M. M., HALLIDAY, A. M., JOHNSON, G., KENDALL, B. E., LOGSDAIL, S. J., and MACMANUS, D. G. (1984): 'NMR in multiple sclerosis and cerebral vascular disease', *Lancet*, **8415**, (2), pp. 1334–1335

PAXINOS, G., and HUANG, X. F. (1995): 'Atlas of the human brainstem' (Academic Press, San Diego)

RUMELHART, D. E., HINTON, G. E., and WILLIAMS, R. J. (1986): 'Learning internal representations by error propagation' in RUMELHART, D. E., and MCCLELLAND, J. L. (Eds): 'Parallel distributed processing: explorations in the microstructure of cognition. Vol. 1, Foundations' (MIT Press, Cambridge, MA), pp. 318–362

SHALTENBRAND, G., and WAHEM, W. (1977): 'Atlas for sterotaxy of the human brain' (Thieme, Stuttgart)

SHARPE, P. K., and CALEB, P. (1994): 'Artificial neural networks within medical decision support systems', *Scand. J. Clin. Lab. Invest. Suppl.*, **219**, pp. 3–11

SIMPSON, P. K. (1990): 'Artificial neural systems' (Pergamon Press, New York)

TURANO, G., JONES, S. J., MILLER, D. H., DU BOULAY, G. H., KAKIGI, R., and MCDONALD, W. I. (1991): 'Correlation of SEP abnormalities with brain and cervical cord MRI in multiple sclerosis', *Brain*, **114** (Pt 1B), pp. 663–81

YANG, T. F., DEVINE, B., and MACFARLANE, P. W. (1994): 'Artificial neural networks for the diagnosis of atrial fibrillation', *Med. Biol. Eng. Comput.*, **32**, (6), pp. 615–619

Author's biography

MARCO CAPOZZA was born in Rome, Italy, in 1955. After graduating *cum laude* in medicine and specialising *cum laude* in neurology, he developed his interest in computational tools. Settling midway between medicine and computer science as a neurologist and a programmer, he is now a research fellow in the School of Neurophysiology, and a lecturer in the Engineering School, in the University of Rome "La Sapienza". His main interests are neural networks, genetic algorithms and nonlinear systems.